Thermochimica Acta, 19 (1977) 161–171

THE CARVOXIME SYSTEM

III. DIFFERENTIAL SCANNING CALORIMETRY EXPERIMENTS: HEATS OF MELTING, PHASE DIAGRAMS AND MELTING BEHAVIOUR OF *dl*-CARVOXIME

H. A. J. OONK, K. H. TJOA, F. E. BRANTS AND J. KROON

Laboratoria voor Structuurchemie en Chemische Thermodynamica, Rijksuniversiteit, Padualaan 8, Utrecht (The Netherlands)

(Received 6 July 1976)

ABSTRACT

Using differential scanning calorimetry (DSC) the solid–liquid equilibria of the system *d*-carvoxime+*l*-carvoxime were investigated. The results confirmed the phase diagram obtained by Adriani, revealed the presence of a continuous series of metastable solid solutions and showed an unusual melting behaviour of *dl*-carvoxime.

Heats of melting and melting points of stable (I) and metastable (II) forms of *l*- and *dl*-carvoxime were measured; they are as follows:

l	I:	$\Delta H = (4.1 \pm 0.1)$ kcal mol^{-1};	*dl*	I:	$\Delta H = (5.3 \pm 0.1)$ kcal mol^{-1}
		$T = (346.1 \pm 0.2)$ K			$T = (364.9 \pm 0.1)$ K
	II:	$\Delta H = (3.3 \pm 0.1)$ kcal mol^{-1}		II:	$\Delta H = (3.6 \pm 0.1)$ kcal mol^{-1}
		$T = (339.6 \pm 0.5)$ K			$T = (353.7 \pm 0.5)$ K

Phase diagram calculations are given as well as a tentative interpretation of the melting behaviour of *dl*-carvoxime.

INTRODUCTION

The phase diagram of *d*-carvoxime+*l*-carvoxime has puzzled an increasing number of scientists ever since its publication by Adriani[1] in 1900. The diagram shown in Fig. 1 is of type II according to Roozeboom's classification[2,3]. The possibility of such a diagram was excluded by Van Laar[4] through thermodynamic reasoning; the validity of his statement, however, is doubtful from the fact that the parameters in his equations for the solid as well as for the liquid state were interpreted in terms of the Van der Waals equation of state.

The phase diagram suggests that in the solid state *l*-molecules can be replaced by *d*-molecules and vice versa. From the point of view of molecular structure this is

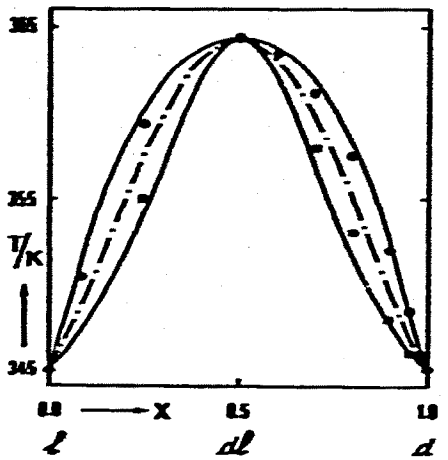

Fig. 1. The solid–liquid equilibrium diagram of the system *d*-carvoxime + *l*-carvoxime. ● and ■, liquidus and solidus points obtained by Adriani[1] from cooling curves; solid lines, calculated phase diagram; dot-dashed line, equal-*G* curve.

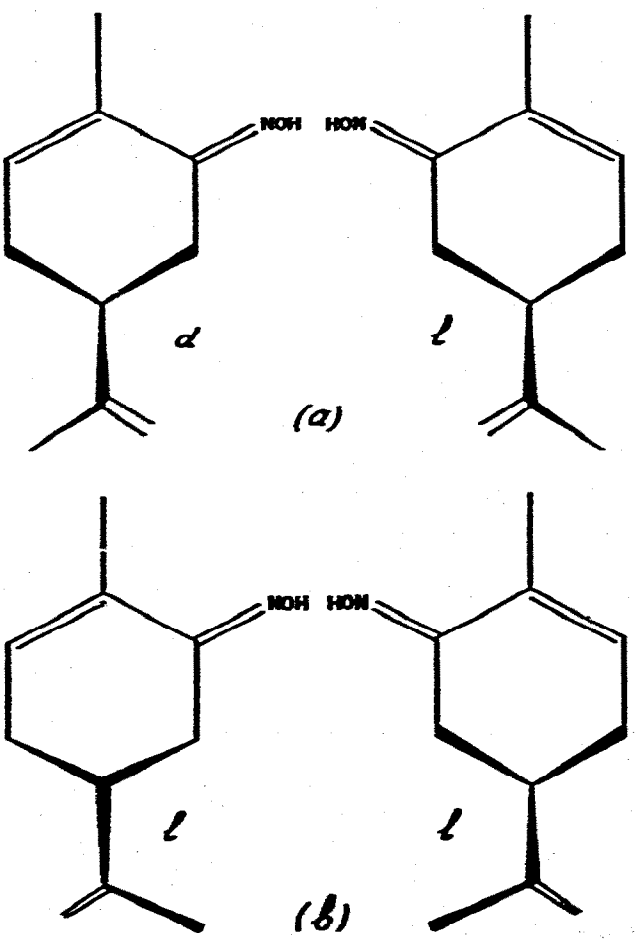

Fig. 2. (a) The *d*- and *l*-molecules in the structure of *dl*-carvoxime[9]. (b) The two independent *l*-molecules in the structure of *l*-carvoxime[8].

plausible: in spite of differences due to molecular asymmetry the *l*- and *d*-molecule are quite planar and therefore similar in their external form (see Fig. 2).

We now propose two simple models for the description of the mixed solid state in the carvoxime system, to be distinguished by the terms *racemate* and *pseudo-racemate*.

In the *racemate* model the 1:1 (the *dl*) composition is an ordered structure in which *d*-molecules are related to *l*-molecules through space group symmetry; they are located on sites which are here to be referred to as *D*- and *L*-sites, respectively. In the direction of an increasing amount of *l*-component, the *d*-molecules on the *D*-sites are randomly replaced by *l*-molecules. In the opposite direction the *L*-sites are gradually filled by *d*-molecules.

In the *pseudoracemate* model the *d*- and *l*-molecules are randomly distributed over the total amount of lattice sites, the 1:1 composition thus has a disordered structure.

It should be noted that, on ignoring the differences between the *d*- and *l*-molecules, the molecular packing scheme is the same for both models and does not change on going from the pure *l*-component via the 1:1 composition to the pure *d*-component. The latter is in accordance with the great similarity in unit-cell dimensions and X-ray reflexion intensities observed for optically active and *dl*-carvoxime[5].

In 1965[5] we expressed our preference for the *pseudoracemate* model mainly because of the equality of entropies of melting, reported by Tammann[6] for *d*-, *l*- and *dl*-carvoxime, and by the observation of some weak X-ray reflexions from *dl*-carvoxime which would have been absent if *dl*-carvoxime were a fully ordered structure.

Some years ago we decided to make a closer study of the carvoxime system. One of the reasons was the pronounced difference in entropies of melting observed by Jacques[7] between optically active and *dl*-carvoxime.

At present, we have completed the crystal structure determinations of *l*-carvoxime (m.p. 345 K) and *dl*-carvoxime (m.p. 365 K)[8,9]. *dl*-Carvoxime proved to have a fully ordered structure with space group $P2_1/c$ instead of pseudo $P2_1/c$ as was assumed in 1965[5]. The weak reflexions mentioned above, which were observed on Weissenberg photographs only, were presumably Renninger reflexions. All this implies that the *pseudoracemate* model cannot be maintained for the solid state corresponding to Fig. 1. To what extent the syncrystallization of *d*- and *l*-molecules can be described by the *racemate* model, is the subject of further investigation.

In this paper we report the results of DSC experiments: heats of melting of *l*- and *dl*-carvoxime, phase diagrams and the melting behaviour of *dl*-carvoxime.

EXPERIMENTAL

Materials

dl- and *l*-carvoxime were prepared from commercial, technically pure, *dl*- and *l*-carvone, respectively. Solutions of carvone and hydroxylamine hydrochloride were

joined and left at room temperature. After three days the reaction mixture was poured into four times its volume of water upon which carvoxime separated. The crude material was recrystallized from methanol. Final purification took place by the rapid zone refining technique described by Bollen[10]; loads of 4 cm^3 having a speed of 6 cm h^{-1} passed through 20 zones.

Methods and results

All experiments described in this contribution were performed on a Perkin-Elmer DSC-2. The samples were weighed on a Mettler microbalance and sealed in small aluminum pans. During these experiments *l*-carvoxime proved to have two solid forms: the higher melting, stable form I and the lower melting, metastable form II. *dl*-Carvoxime can assume several solid forms, two of these correspond to forms I and II of *l*-carvoxime; see Table 1 for melting points.

TABLE 1

THERMODYNAMIC QUANTITIES OF THE CARVOXIME SYSTEM

	l/*dl*	*Form II*	*Form I*
Melting points (K)	*l*	339.6±0.5	346.1±0.2
	dl	353.7±0.5	364.9±0.1
Enthalpies of melting (kcal mol^{-1})	*l*	3.3±0.1	4.1±0.1
			3.87[a]
			3.9[b]
	dl	3.6±0.1	5.3±0.1
			4.06[a]
			5.3[b]
Parameters of eqn (11)			
a		270	390
			420[c]
b		1080	2000
			2000[c]
Difference excess quantities at $X=\frac{1}{2}$ (cal mol^{-1})			
ΔH^E		300	1200
$T\Delta S^E$		163	877
ΔG^E		137	223

[a] Tammann[6] from cooling curves. [b] Jacques[7] by DSC. [c] Corresponding to Fig. 1.

Heat effects. The pulvarized samples (0.5–3 mg) were scanned at a heating rate of 5 K min^{-1}. Peak areas were either measured by means of an Ott planimeter or registered on a Kipp integrator, BC-1, attached to the DSC. A continuous baseline was assumed. Using zone refined naphtalene and indium standards, the heats of melting were calculated from the peak areas; the mean results of many determinations are given in Table 1. Scans of *l*-carvoxime showed either peaks of form I or forms I

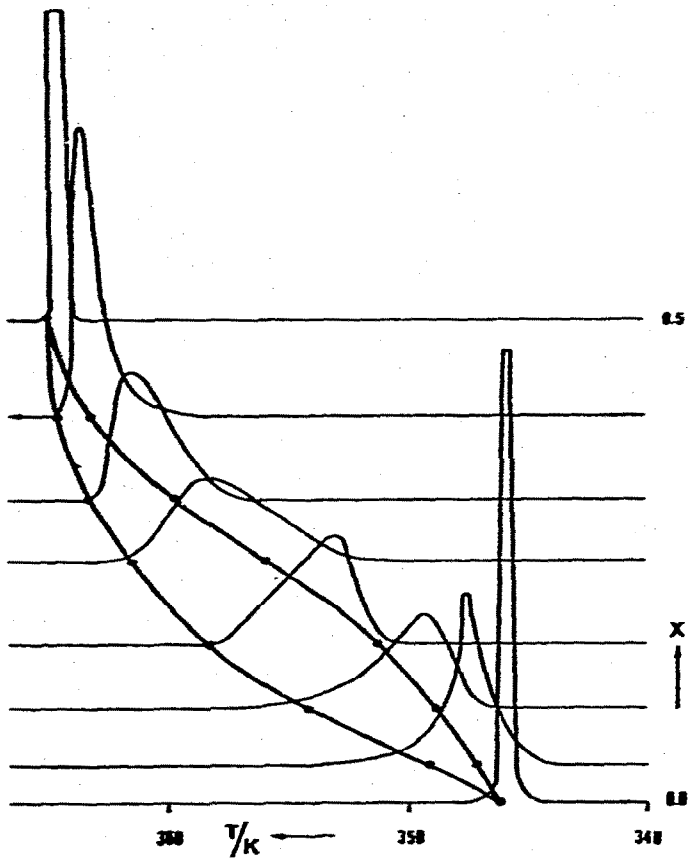

Fig. 3. The calculated phase diagram corresponding to DSC observations. The inserted scans illustrate the possibilities of this method. Dots are calculated points of the same respective mole fractions as the samples.

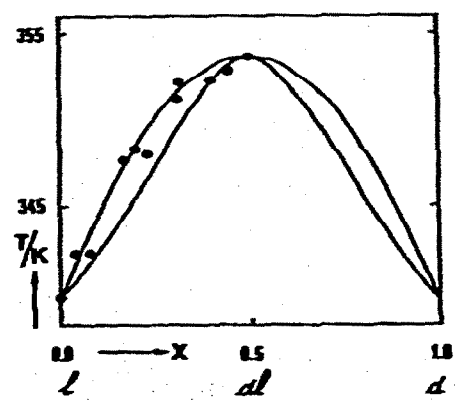

Fig. 4. The solid–liquid equilibrium diagram of the metastable series of solid solutions, as revealed by DSC experiments. ●, experimental liquidus points; solid lines, the calculated diagram.

and II combined, so that the value of *l*-carvoxime II had to be calculated using the value for I. However, samples of non-zone refined material did show single peaks at 339.6 K.

Phase diagrams. Samples containing *l*- and *dl*-carvoxime in varying amounts, from which the mole fractions are calculated, had a total weight of ca. 2 mg.

To determine the *T–X* phase diagram of the stable form a heating rate of 0.31 K min^{-1} was used. This could not be applied to the metastable forms which did not manifest themselves at this low rate; instead efforts resulted in the appearance of an exothermic peak below the melting point, after which the sample melted as in the stable structure. Therefore, a heating rate of 5 K min^{-1} was used although this meant a greater uncertainty in the points.

Each sample was first heated to 370 K, the resulting peak reached from the melting point of the pure *l*-component to that of the *dl*-composition. The subsequent scans were used for the determination of the phase diagrams.

The results of the experiments are given in Figs. 3 and 4.

Melting behaviour of dl-carvoxime. Samples consisting of different amounts of *dl*-carvoxime were heated at a rate of 5 K min^{-1}. Each sample was scanned and cooled several times with periods between scans varying from several minutes to several weeks. The following types of scans were noted, see Fig. 5, all in the 351–365 K range: (a) one sharp peak; (b) one main peak supplemented with one, two or three minor peaks; (c) as (b), with an additional exothermic peak.

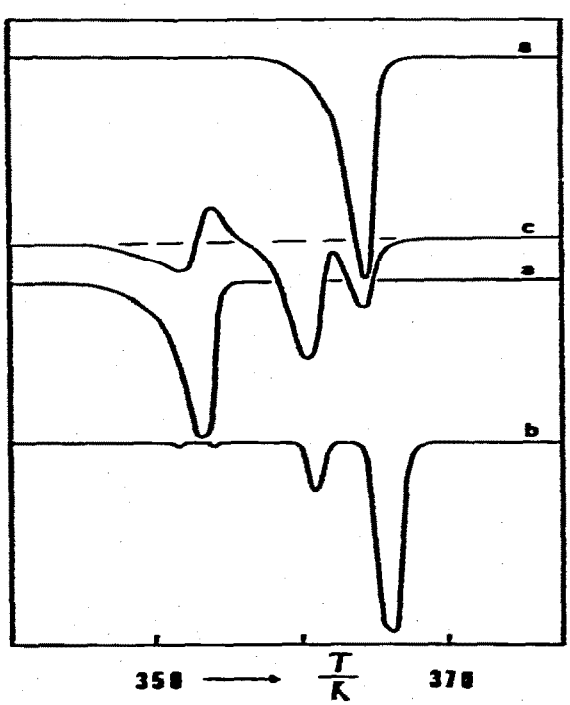

Fig. 5. DSC scans illustrating the unusual melting behaviour of *dl*-carvoxime. The letters a, b, and c correspond to the types described in the section *Methods and results*.

Experiments were also done on material recrystallized from methanol, with similar results; however, supplementary peaks were repeatedly found below 351 K down to 347 K.

Peak areas were measured with an Ott planimeter and heat effects calculated as before.

For scans of type (a), heats of melting are plotted against the melting temperature, see Fig. 6. The distribution of peaks from 29 scans of zone refined material is shown on the abscissa of Fig. 6.

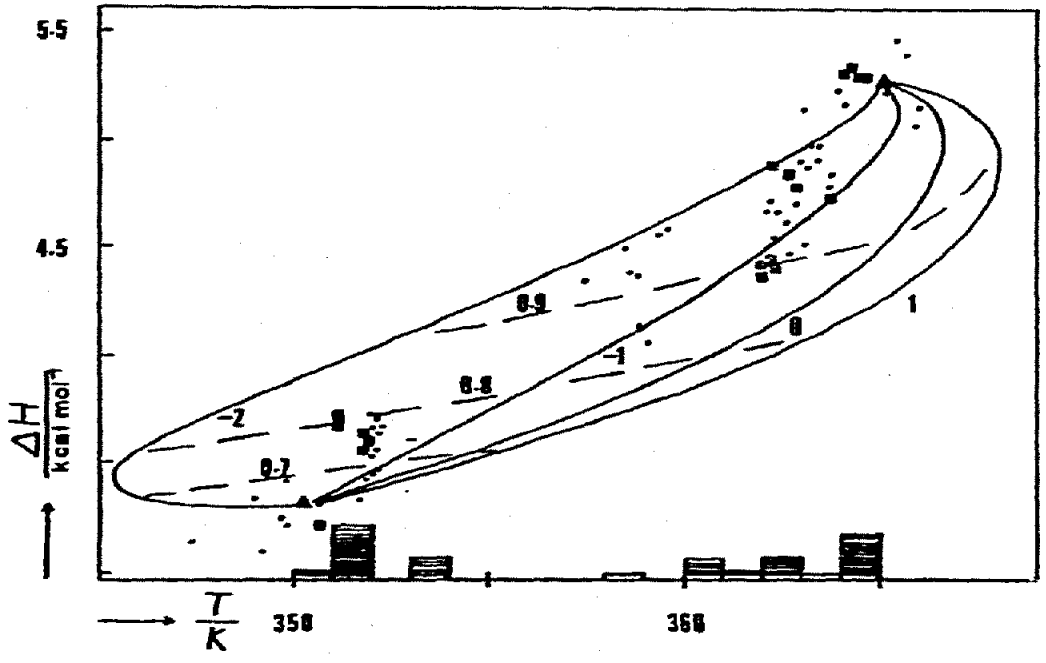

Fig. 6. The melting behaviour of *dl*-carvoxime: heats of melting plotted against melting temperature. ■ and ●, experimental points of type (a) obtained from zone refined material and material recrystallized from solution, respectively; solid lines, theoretical curves corresponding to the values of parameter $a_1 = a_2 = 1, 0, -1, -2$ in eqns (19) and (20); dashed lines, join points of equal order r, the value of which is indicated. The distribution of all peaks observed in 29 DSC scans on four samples of zone refined material is given along the abscissa.

The results in Fig. 6 show that *dl*-carvoxime can assume several solid forms, of which the heats of melting increase with melting point.

In the second part of the following section a theoretical analysis of the melting behaviour observed is given; it is based on the assumption that *dl*-carvoxime exhibits a continuous series of solid forms from 350 to 365 K.

CALCULATIONS AND CONCLUSIONS

Phase diagrams

The Gibbs energy of liquid mixtures of optical antipodes, consisting of X moles of *d*-molecules and $(1-X)$ moles of *l*-molecules, is given by the following expression

in temperature T and mole fraction X

$$G^{liq}(T, X) = X\mu_d^{*liq}(T) + (1-X)\mu_l^{*liq}(T) + RT\,\mathrm{LN}(X) + G^{Eliq}(T, X) \quad (1)$$

where

$$\mathrm{LN}(X) = (1-X)\ln(1-X) + X\ln X \quad (2)$$

and G^E denotes the excess Gibbs energy, i.e., gives the deviation from ideal solution behaviour.

The molar Gibbs energies of both pure *d*- and *l*-components, μ_d^* and μ_l^*, are equal, from which eqn (1) may be rewritten as

$$G^{liq}(T, X) = G^{*liq}(T) + RT\,\mathrm{LN}(X) + G^{Eliq}(T, X) \quad (3)$$

Neglecting C_p influences and separating G^* and G^E into enthalpy H and entropy S parts, eqn (3) becomes

$$G^{liq}(T, X) = H^{*liq} - TS^{*liq} + RT\,\mathrm{LN}(X) + H^{Eliq}(X) - TS^{liqE}(X) \quad (4)$$

where H^* and S^* are constants and H^E and S^E are independent of T.

The same expressions are used for the solid state, although in the *racemate* model the contribution from substitutional disorder is certainly not represented by $RT\,\mathrm{LN}(X)$.

$$G^{sol}(T, X) = H^{*sol} - TS^{*sol} + RT\,\mathrm{LN}(X) + H^{Esol}(X) - TS^{Esol}(X) \quad (5)$$

The intersection of the G^{sol} and G^{liq} surfaces is given by

$$\Delta G \equiv G^{liq} - G^{sol} = 0 \quad (6)$$

Note: The difference function is defined by $\Delta f \equiv f^{liq} - f^{sol}$ where f stands for H, G, S etc.

Substitution of eqns (4) and (5) into eqn (6) yields

$$\Delta H^* - T\Delta S^* + \Delta H^E(X) - T\Delta S^E(X) = 0 \quad (7)$$

The equal-G curve[11], the projection of the intersection on the TX plane, using eqn (7) is given by

$$T_{EGC}(X) = \frac{\Delta H^* + \Delta H^E(X)}{\Delta S^* + \Delta S^E(X)} \quad (8)$$

In eqn (7) the excess part represents the excess Gibbs energy along the EGC

$$\Delta H^E(X) - T_{EGC}\Delta S^E(X) = \Delta G^E_{EGC}(X) \quad (9)$$

Substituting eqn (9) into eqn (7), eqn (8) is implicitly given by

$$T_{EGC}(X) = \frac{\Delta H^*}{\Delta S^*} + \frac{\Delta G^E_{EGC}(X)}{\Delta S^*} = T_0 + \frac{\Delta G^E_{EGC}(X)}{\Delta S^*} \quad (10)$$

T_0 signifying the melting point of the pure antipodes.

The procedure used for the calculation of the phase diagram is as follows:

ΔG^E is represented by the following expression in X

$$\Delta G^E_{EGC}(X) = aX(1-X)+bX^2(1-X)^2 \qquad (11)$$

The equal-G curve has the general property of lying between solidus and liquidus, see Fig. 1. In the experimental phase diagram a curve is drawn which is expected to be a good representative of the real EGC. Using eqns (10) and (11), the values of the constants a and b are determined, from which an approximate phase diagram is calculated[12]. Next the values of a and b are adapted until agreement between the calculated and experimental liquidus is obtained.

Note that as the experimental ΔG^E cannot be separated into G^{Eliq} and G^{Esol}, ($\Delta G^E = G^{Eliq} - G^{Esol}$), the phase diagram calculations were performed assuming an ideal liquid state, which is believed to be a good approximation for antipode systems[13]; consequently $G^{Esol} = -\Delta G^E$.

The values found for the parameters a and b are indicated in Table 1; the calculated phase diagrams are plotted in Figs. 3 and 4.

For the diagram in Fig. 3, G^{Esol} was separated into enthalpy and entropy parts having the same dependence on X as G^{Esol}, cf., Table 1.

Melting behaviour of dl-carvoxime

Molecules of *d*- and *l*-carvoxime form two series of solid solutions, the higher melting series I and the lower melting series II. From structure determinations, there is strong evidence that in series I the substitution of molecules is of the *racemate* type[9]; it is accompanied with pronounced changes in the conformational arrangement of the isopropenyl group[8,9].

We now expect that the substitution in series II is of the *pseudoracemate* type, the molecular packing scheme being the same as in series I. This implies that we expect the difference between the forms I and II of *l*-carvoxime to be due to differences in molecular conformation or to conformational disorder or both, and the difference between forms I and II of *dl*-carvoxime to be the combined result of conformational changes and substitutional disorder.

In this view *dl* I and *dl* II are the beginning and the end of a series of structures, either continuous or with discrete intermediates, having a varying degree of substitutional order.

This may be expressed in terms of an order parameter r denoting the fraction of *D*-sites occupied by *d*-molecules which is equal to the fraction of *L*-sites occupied by *l*-molecules; $r = \frac{1}{2}$ indicates the *pseudoracemate* and $r = 1$ the *racemate*.

For the *dl*-composition we now assume that the Gibbs energy may be given by the following continuous function in T and r

$$G^{sol}(T, r) = G^{*sol}(r=1) + RT\,\mathrm{LN}(r) + G^{"E"sol}(r) \qquad (12)$$

where

$$\mathrm{LN}(r) = r\ln r + (1-r)\ln(1-r) \qquad (13)$$

it results from the number of possible configurations with given r (ref. 5).

The last term $G^{\overline{E}sol}$, an excess Gibbs energy, is analogous to the term indicating the deviation from ideal solution behaviour as given in the phase diagram calculations. The variable X, however, has been replaced by r.

Separating $G^{sol}(T, r)$ into enthalpy and entropy parts, assumed to be independent of temperature, eqn (12) becomes

$$G^{sol}(T, r) = H^{*sol} - TS^{*sol} + RT \text{ LN}(r) + H^{\overline{E}}(r) - TS^{\overline{E}}(r) \tag{14}$$

As before an ideal liquid state is assumed; its Gibbs energy is a function of T

$$G^{liq}(T, r) = H^{*liq} - TS^{*liq} \tag{15}$$

The intersection of G^{sol} and G^{liq} is given by

$$\Delta G \equiv G^{liq} - G^{sol} = 0 \tag{16}$$

Substitution of eqns (14) and (15) into eqn (16) gives

$$\Delta H^* - T\Delta S^* - RT \text{ LN}(r) - H^{\overline{E}} + TS^{\overline{E}} = 0 \tag{17}$$

from which the melting points as a function of r, are given by

$$T(r) = \frac{\Delta H^* - H^{\overline{E}}}{\Delta S^* + R \text{ LN}(r) - S^{\overline{E}}} \tag{18}$$

Parallel to the treatment applied in the previous calculations, the excess functions are represented by

$$H^{\overline{E}} = \omega\{r(1-r) + a_1 r^2(1-r)^2\} \tag{19}$$

$$S^{\overline{E}} = \sigma\{r(1-r) + a_2 r^2(1-r)^2\} \tag{20}$$

in which ω and σ are constants of dimensions cal mol^{-1} and cal mol^{-1} K^{-1}, respectively; a_1 and a_2 are dimensionless parameters.

The values of ω and σ for given values of a_1 and a_2 follow from the enthalpies of melting and the melting points of forms I (the *racemate*) and II (the *pseudo-racemate*). With these values the numerator of eqn (18), ΔH, may be calculated and plotted against T, obtained from eqn (18) and at a chosen r. The result is given in Fig. 6, for which $a_1 = a_2 = a$ and the following experimental values were used

$$\Delta H(r = 1) = 5300 \text{ cal mol}^{-1} \qquad \Delta H(r = \tfrac{1}{2}) = 3300 \text{ cal mol}^{-1}$$

$$T(r = 1) = 365 \text{ K} \qquad T(r = \tfrac{1}{2}) = 350 \text{ K}$$

The theoretical curves are for $a = 1, 0, -1, -2$.

One final remark: if our model is valid, the melting point of *dl*-carvoxime prepared by equilibrium crystallization from a solution (in, e.g., methanol) will be expected to depend on the temperature of crystallization, for the equilibrium value of r follows from the condition $\partial G/\partial r = 0$ applied to eqn (12), upon which the melting point follows from eqn (18).

For example for $a = -1$ crystallization at 300 K corresponds to an equilibrium value of $r = 0.9996$ and a melting point of 365.08 K, for crystallization at 360 K these values will be $r = 0.9917$ and $T = 365.48$ K, respectively.

REFERENCES

1 J. H. Adriani, *Z. Phys. Chem.*, 33 (1900) 453.
2 H. W. Bakhuis Roozeboom, *Z. Phys. Chem.*, 8 (1891) 504.
3 H. W. Bakhuis Roozeboom, *Z. Phys. Chem.*, 28 (1899) 494.
4 J. J. van Laar, *Z. Phys. Chem.*, 64 (1908) 289.
5 H. A. J. Oonk, *Thesis*, Utrecht (1965).
6 G. Tammann, *Z. Phys. Chem.*, 87 (1914) 357.
7 J. Jacques, personal communication (1968) and J. Jacques and J. Gabard, *Bull. Soc. Chim. Fr.*, (1972) 342.
8 J. Kroon, P. R. E. van Gurp, H. A. J. Oonk, F. Baert and R. Fouret, *Acta Crystallogr. B*, 32 (1976) 2561.
9 H. A. J. Oonk and J. Kroon, *Acta Crystallogr. B*, 32 (1976) 500.
10 N. J. G. Bollen, M. J. van Essen and W. M. Smit, *Anal. Chim. Acta*, 38 (1967) 279.
11 H. A. J. Oonk, *Rec. Trav. Chim.*, 87 (1968) 1345.
12 H. A. J. Oonk, *J. Chem. Educ.*, 47 (1970) 227.
13 K. Amaya, *Bull. Chem. Soc. Japan*, 34 (1961) 1689.